

# Boundary Layer Measurements on an Airfoil at a Low Reynolds Number in an Oscillating Freestream

M. Brendel\* and T. J. Mueller†

*University of Notre Dame, Notre Dame, Indiana*

The influence of a periodic nonreversing wind-tunnel flow on an airfoil operating at low chord Reynolds numbers is investigated. The focus of this work was on the temporal behavior of the transitional separation bubbles that occur on a Wortmann FX63-137 airfoil at low speeds. Unsteady pressure distributions and flow visualization were used to determine if periodic bubble bursting would result from large-amplitude periodic fluctuations in the chord Reynolds number. It was found that the transitional bubble remained intact even when the instantaneous chord Reynolds number was below the steady-flow bubble-bursting freestream speed (critical Reynolds number). The cause of this is connected with a flow hysteresis that is a function of changes in chord Reynolds number. In more detailed experiments, mean unsteady and phase-locked velocity profiles were obtained using hot-wire anemometry for an unsteady flow having an oscillation period of 0.5 s, an amplitude of 7% of the mean flow, and a mean chord Reynolds number of 100,000. The mean unsteady displacement thicknesses in the laminar portion of the transitional separation bubble were lower than the steady values while the mean unsteady momentum thicknesses did not show significant differences. Downstream of transition and reattachment, the mean unsteady momentum thicknesses were less than the corresponding steady-flow values. In addition, the chord-wise location of maximum displacement appeared to move downstream when the external flow velocity was increasing. These results suggested that transition was suppressed during the accelerating portion of the unsteady flow cycle.

## Nomenclature

- $A$  = oscillation amplitude ratio,  $\Delta U_\infty/U_\infty$   
 $C_p$  = pressure coefficient,  $1 - q/q_\infty$   
 $c$  = airfoil chord  
 $f$  = oscillation frequency,  $1/\tau$   
 $k_c$  = reduced frequency,  $fc/U_\infty$   
 $k_x$  = reduced frequency,  $fx/U_\infty$   
 $q_\infty$  = mean freestream dynamic pressure  
 $R_c$  = mean Reynolds number, chord,  $U_\infty c/\nu$   
 $q$  = dynamic pressure  
 $t$  = time  
 $U$  = reference velocity  
 $u$  = local velocity  
 $x$  = distance from leading edge (along chord line)  
 $\Delta$  = amplitude of fluctuating component (i.e.,  $\Delta u$ )  
 $\delta$  = boundary layer thickness
- $\delta_1$  = displacement thickness,  $\int_0^\delta \left(1 - \frac{u}{U_e}\right) dy$   
 $\delta_2$  = momentum thickness,  $\int_0^\delta \frac{u}{U_e} \left(1 - \frac{u}{U_e}\right) dy$
- $\rho$  = density  
 $\tau$  = oscillation period,  $1/f$   
 $\nu$  = kinematic viscosity  
 $\phi$  = phase angle between local and external velocity,  $\phi_1 - \phi_\infty$

## Subscripts

- $e$  = external to boundary layer  
 $s$  = separation

- $t$  = transition  
 $\infty$  = freestream quantity  
 $l$  = local quantity

## Introduction

THE dependence of airfoil performance on chord Reynolds number in incompressible flow has been known for many years.<sup>1,2,3</sup> Recently, the performance of airfoils operating at chord Reynolds numbers below 500,000 has been of interest for a variety of applications including remotely piloted vehicles, sailplanes, human-powered vehicles, leading-edge control devices, high-altitude vehicles, wind turbines, and propellers.<sup>4</sup> In contrast to boundary layers at higher Reynolds numbers, the low Reynolds number airfoil boundary layer often remains laminar well into the pressure recovery region and laminar separation usually takes place with transition to turbulence occurring in the separated shear layer. After transition, the turbulent mixing may be sufficient to eliminate the reverse flow downstream of separation by causing the turbulent shear layer to reattach to the surface. This "closed" region, conceptually modeled in Fig. 1, is the transitional separation bubble. The bubble may be large enough to alter the effective geometry of the airfoil and thus alter the predicted pressure distribution. Transitional bubbles form at higher Reynolds numbers, but generally have little influence on the overall pressure distribution since they only occupy a small percentage of the chord length (<5% typ.). In contrast, a bubble that extends over 15% of chord is not uncommon at chord Reynolds numbers below 300,000. Predicting the formation and extent of a transitional bubble has been one of the most difficult problems in boundary-layer research.

Most analytical and experimental studies of low Reynolds number aerodynamics have focused on steady-flow performance.<sup>4</sup> In practice, the operating environment of any flight vehicle includes unsteady conditions that may be due to vehicle dynamics (e.g., phugoid, short period), vehicle aerodynamics (e.g., wing-stabilizer interference), or of external origin (e.g., downburst, longitudinal gusts). Periodic or transient motions of lifting surfaces in steady flow have been studied for many

Received April 3, 1987; presented as Paper 87-1332 at the AIAA 19th Fluid Dynamics, Plasma Dynamics, and Laser Conference, Honolulu, HI, June 8-10, 1987; revision received Sept. 25, 1987. Copyright © 1987 by T. J. Mueller. Published by the American Institute of Aeronautics and Astronautics, Inc., with permission.

\*Research Associate, Visiting Assistant Professor, Aerospace and Mechanical Engineering Department. Member AIAA.

†Professor, Aerospace and Mechanical Engineering Department. Associate Fellow AIAA.

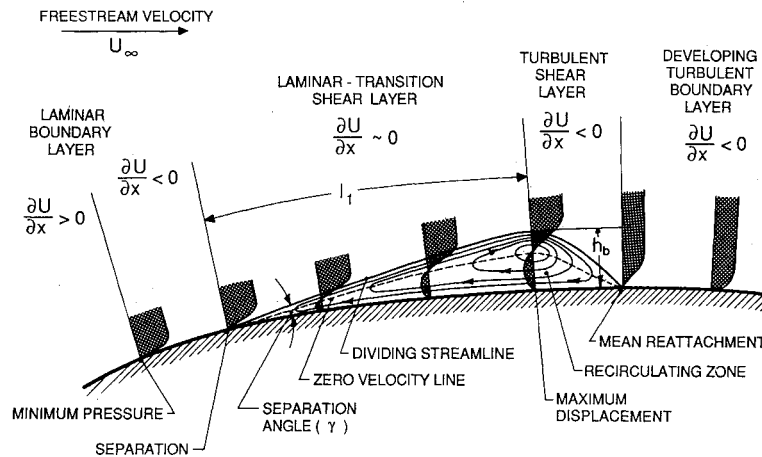


Fig. 1 Mean conceptual features of a transitional separation bubble.

years.<sup>5</sup> However, relatively few studies have addressed the effect of unsteady flows on stationary lifting surfaces. Low-altitude remotely piloted vehicles operate in the atmospheric boundary layer where the local wind fluctuations or the vertical wind shear may be comparable to the vehicle air speed. Predicting the stability of a vehicle operating in an unsteady environment requires the aerodynamic response to flow unsteadiness. The form of unsteadiness encountered in actual flight conditions will tend to vary in a complicated, and unpredictable manner. However, controlled wind-tunnel experiments can be devised to study the influence of specific forms of unsteady flow in order to isolate dominant effects.

The boundary layer on a Wortmann FX63-137 airfoil was studied in both steady flow and nonreversing stream-wise periodic flow. Unsteady pressure distributions were obtained to investigate the possibility of intermittent separation of the boundary layer in response to the periodic external flow. Although these results did not indicate any unusual behavior for the cases studied, the consequences of "quasisteady" periodic flows on airfoil performance and some additional insight into the lift hysteresis phenomena were revealed. Phase-locked hot-wire velocity profiles were obtained for a mean chord Reynolds number of 100,000 ( $U_\infty \sim 5.2$  m/s) with a 2 Hz sinusoidal variation in the freestream and an amplitude ratio  $A$ , 7% of the mean flow speed. This represented a wavelength of 8.5 chord lengths, or a reduced frequency  $k_c = fc/U_\infty$  of 0.11. Previous experimental work of this type was limited to larger Reynolds numbers, incidence angles near stall,<sup>6,7</sup> or airfoils moving in translation.<sup>8</sup> The hot-wire surveys served to compare the boundary layer characteristics in steady and unsteady flow conditions.

### Apparatus

The wind tunnel used in these experiments was an in-draft no-return type (atmospheric exhaust) with the following configuration: a 24:1 inlet contraction with 12 antiturbulence screens; an interchangeable 0.61 m  $\times$  0.61 m cross-section working section; a 4.2-m-long diffuser with 4.2 deg included angle divergence; and an 18.6 kW AC motor directly coupled to a 1.2 m (48 in.) diam fan. In order to produce an oscillating freestream, a special unsteady-flow generator was constructed and adapted to the existing subsonic wind tunnel. An unsteady velocity was produced by the pitching motion of four 610  $\times$  150  $\times$  6 mm (24  $\times$  6  $\times$  0.25 in.) louvers mounted horizontally across the flow channel. The louvers were driven by a DC servo motor that was controlled by a microcomputer. In the present experiments, a nonreversing stream-wise periodic velocity was produced by oscillating the louvers about a fixed position. This method was used since it resulted in a velocity waveform with low harmonic distortion relative to rotating the

louvers at constant speed. Nonetheless, a technique to further reduce harmonic distortion of velocity variation was developed and employed throughout these experiments. Through the use of computer control, the velocity waveform in the test section had excellent repeatability and less than 4% total harmonic distortion in amplitude (0.2% spectral energy). Measured RMS velocities, nondimensionalized by the mean freestream velocity in the test section, were less than 0.08% in both the steady and unsteady flow for a bandwidth of 10 to 2500 Hz. Steady-flow tests were conducted with the unsteady-flow generator in place, and louvers fixed, to insure that any facility-related disturbances would be consistent in both the steady and unsteady flows.

Two cast epoxy-resin airfoil models with chords of 305 mm and spans of about 400 mm were used in the present experiments. The model was mounted between two endplates in the center of the test section. The pressure model had 96 pressure taps that were connected through two scanivalves to an electronic manometer (0–1.37 kPa, 5 in. H<sub>2</sub>O). Pressure measurements were intended only to reveal major features of the boundary layer such as massive separation. The long, small-diameter tubing used in this model resulted in a very poor frequency response of the system ( $-3$  dB @ 2.5 Hz). Boundary-layer velocity measurements were obtained on the second model using a constant-temperature anemometer with a single-sensor (5  $\mu$ m diam) boundary layer probe. The thin region of interest ( $\sim 3$  mm thick) precluded the use of multisensor probes. A second hot-wire sensor was placed upstream of the airfoil model to provide a phase reference for both the hot-wire and pressure experiments. All data acquisition and processing were performed digitally on a microcomputer. A schematic of the test arrangement is shown in Fig. 2. All data acquisition was phase-locked to the motion of the louvers producing the unsteady flow. Further description of the apparatus and data processing techniques may be found in Ref. 9. A list of uncertainty estimates associated with these apparatus are listed in Table 1.

Since these experiments relied heavily upon automated data acquisition, a benchmark experiment was performed in order to test the operation of the unsteady facility and the data acquisition/processing techniques. The unsteady laminar boundary layer on a flat plate was examined using flow conditions identical to those used in the airfoil experiments. The plate was fabricated from tooling aluminum and was 610 mm (24 in.) wide, 1200 mm (48 in.) long, and 10 mm (0.38 in.) thick with an elliptic leading edge. A trailing edge flap was used to adjust the pressure distribution. Also, the flap served to keep the front stagnation point on the upper surface and thus prevent a leading-edge separation bubble. Results of the benchmark test formed a basis for comparison and also verified the experimental method.

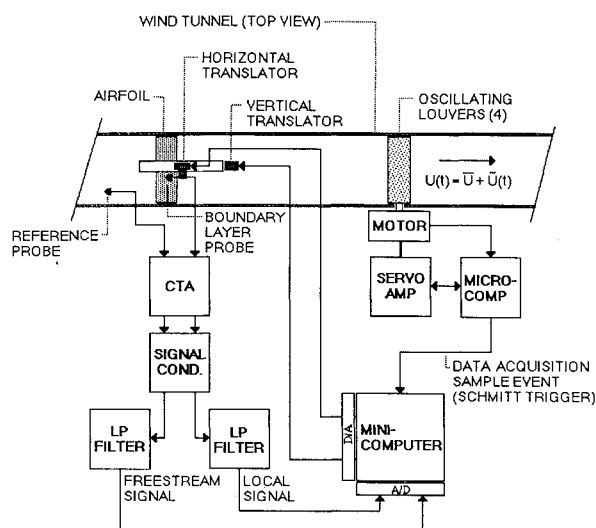


Fig. 2 Schematic of the test apparatus.

Table 1 Uncertainty estimates

Separation $S$	$\pm 0.5\%$ chord
Transition $T$	$\pm 1.5\%$ chord
Reattachment $R$	$\pm 3.0\%$ chord
Displacement thickness $\delta_1$	$< 0.1$ mm
Momentum thickness $\delta_2$	$< 0.05$ mm
Phase $\phi$	$< 5$ deg
Normal distance from airfoil	$\pm 0.2$ mm
Velocity ratio $u/U_\infty$	$< 5\%$ typical

## Results

Two aspects of unsteady flow over the Wortmann airfoil are presented. The first involves the implications of the "quasi-steady" response of the airfoil boundary layer. Here, pressure distribution data revealed a consequence of flowfield unsteadiness that offers some insight into the lift hysteresis phenomenon. In the discussion of hot-wire results a distinction is made between mean unsteady and steady data. Both are calculated as arithmetic averages with the only difference being the base flow, unsteady or steady, in which the data were obtained. The fluctuating velocity ratio  $\Delta u/\Delta U_e$  was determined from the oscillation amplitudes of the respective velocities, and phase  $\phi = \phi_l - \phi_\infty$  was computed from the Fourier transform of the local and external velocity fluctuations at the base flow frequency (2 Hz).

### Benchmark Tests

An important result of numerous oscillating boundary-layer studies has been that the mean unsteady velocity profile was the same as the steady velocity profile even in flow with relatively large fluctuation amplitude (30% in Ref. 10 for a turbulent boundary layer).<sup>10-12</sup> The benchmark test described above produced the same result. In addition, the behavior of phase angle  $\phi$  and fluctuating velocity ratio  $\Delta u/\Delta U_e$  was as expected for variations in reduced frequency  $k_x$ . These results justified the data acquisition/reduction techniques used in the unsteady-flow experiments.

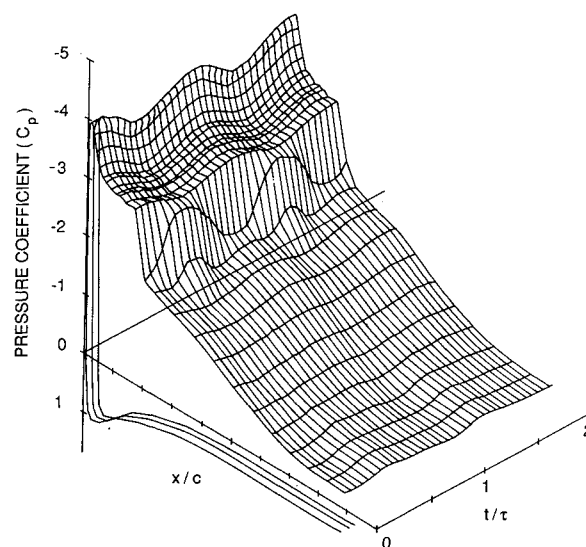
### Pressure

It is well known that lift hysteresis may occur as a function of increasing and decreasing incidence in a steady free-stream.<sup>13,3,4</sup> This type of hysteresis is generally associated with the formation, location, and bursting of a transitional separation bubble as a function of incidence. Typically, bursting occurs when the separated turbulent shear layer can no longer

overcome the adverse pressure gradient required to reattach, or turbulent separation moves forward from the trailing edge and "interferes" with the reattaching portion of the bubble. However, there is a similar phenomenon that occurs with changes in chord Reynolds number at a fixed incidence angle. For this case, there is a critical Reynolds number below which hysteresis does not occur due to the initial lack of a transitional bubble formation. The critical Reynolds number for the Wortmann section was determined to be about 70,000. This suggests the possibility of an intermittent separation bubble if the flow oscillates such that the instantaneous Reynolds number falls below the critical value during a portion of the cycle (i.e., the incidence is fixed within the hysteresis loop). A test of this type was performed with the Wortmann airfoil at 15 deg angle of attack, a mean chord Reynolds number of 80,000, and an amplitude  $A$  of 19%. The flow remained attached to the upper surface, which corresponded to the upper branch of the hysteresis loop. The minimum instantaneous Reynolds number was about 65,000. (Note: when the wind-tunnel speed is accelerated to a steady flow at  $R_c = 65,000$ , complete separation from the upper surface occurs at this angle of attack.) The result, shown in Fig. 3, indicates that there was a transitional bubble throughout each cycle (i.e., completely separated flow would be indicated by a collapse of the pressure distribution). The separated shear layer, characterized by the pressure plateau downstream of minimum pressure, can be seen to lengthen with decreasing velocity as would be expected for a quasisteady flow (i.e., transition length increases). This behavior has some important implications which, in hindsight, were not surprising.

Steady-flow force measurements conducted by changing the angle of attack in a fixed velocity stream, the "polar" method, cannot be used in a quasisteady analysis for Reynolds number variations near the critical value. This was first recognized by Schmitz,<sup>3</sup> but has received little attention since. The reader is directed to Ref. 14 that contains experimental results using both methods as originally reported in Ref. 3. Not only is there a hysteresis with changes in incidence, but also a hysteresis in Reynolds number variations, "the characteristic" method, as illustrated in Fig. 4.

The reason for the hysteresis is connected with the mechanism of transition and the pressure distribution. Once a bubble has burst, there is insufficient pressure recovery of the turbulent shear layer and the pressure distribution collapses. It follows that the separation location, momentum thickness, and external velocity changes. This alters the stability characteristics of

Fig. 3 Temporal development of the pressure distribution (mean  $R_c = 80,000$ ,  $k_c = 0.04$ ,  $A = 19\%$ ).

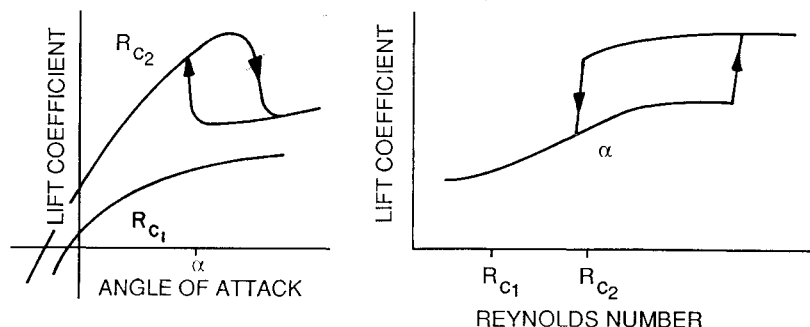


Fig. 4 Illustration of the lift hysteresis as a function of Reynolds number.

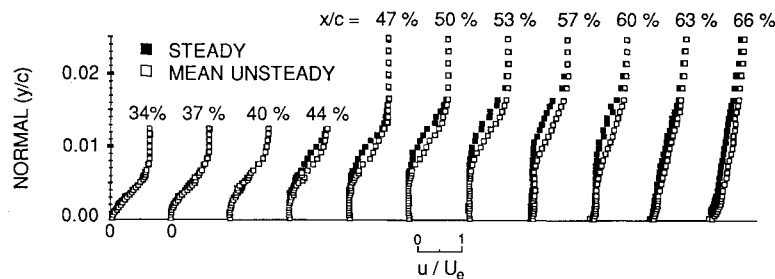


Fig. 5 Comparison of the steady and mean unsteady velocity profiles in the vicinity of the separation bubble (Wortmann FX63-137 airfoil;  $\alpha = 7$  deg,  $R_c = 100,000$ ;  $k_c = 0.11$ ;  $A = 7\%$  [ $c = 305$  mm/12 in.]).

the separated shear layer to a degree that does not allow reattachment until transition can occur relatively near the surface. One can consider that the decreased velocity at separation, relative to the situation with a bubble, results in a longer laminar portion of the shear layer. By the time transition occurs, the displacement is too great to reattach. In order for the shear layer to reattach again, the external velocity must be increased (i.e., more energy) or incidence decreased (i.e., less pressure gradient) to move transition closer to the surface, hence, allowing reattachment and reformation of the bubble pressure distribution. This could be done artificially by forcing the separated layer to transition early. A sharp blow to the wind-tunnel inlet nozzle with a rubber mallet was sufficient to force the flow to reattach to the surface. These observations are pertinent to steady or quasisteady flow and do not show any true time dependence. However, it was the unsteady flow that revealed this behavior.

#### Hot-Wire Measurements

Hot-wire velocity profile measurements were obtained at a mean chord Reynolds number of 100,000 for several angles of attack. The unsteady flow had a frequency of 2 Hz,  $k_c = 0.11$ , and an amplitude ratio  $A$  of about 7%. Results from the 7 deg angle-of-attack condition are representative and are presented here. Figure 5 is a comparison of mean velocity profiles in the steady- and unsteady-flow conditions in the vicinity of the transitional bubble. The mean unsteady profiles and steady profiles were nearly the same up to, and including, laminar separation (about 33% of chord; determined from flow visualization and chord-wise extrapolation of measured profiles, separation occurred at the same location in the steady and mean unsteady flow within uncertainty of this measurement<sup>15</sup>). In the laminar portion of the bubble, however, the mean trajectory of the unsteady separated shear layer was found to be closer to the airfoil surface than in the steady flow. It should be noted that the mean external velocities were similar in both flows. The "thinning" of the separated shear layer is reflected in the mean chord-wise development of the displacement thickness  $\delta_1$ , shown in Fig. 6. In addition, it was found that the instantaneous displacement thickness never exceeded the steady value. Phenomena of this type have been observed in other unsteady boundary layer flows.<sup>16,17</sup>

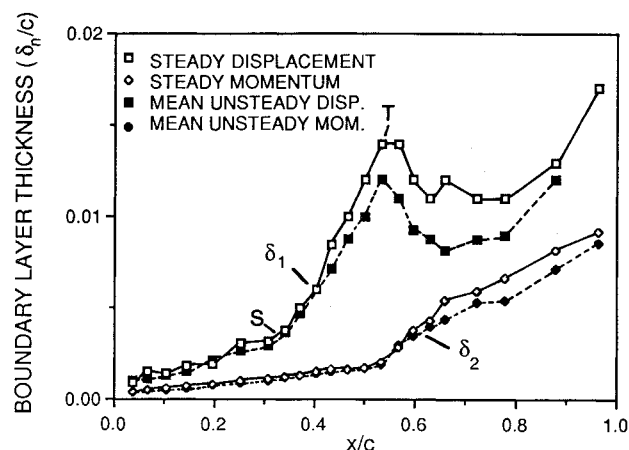


Fig. 6 Comparison of the steady and mean unsteady displacement and momentum thicknesses (Wortmann FX63-137 airfoil;  $\alpha = 7$  deg,  $R_c = 100,000$ ;  $k_c = 0.11$ ,  $A = 7\%$  [ $c = 305$  mm/12 in.]).

The maximum measured displacement of the bubble was used as an indicator for transition. This corresponded to a sharp increase in the momentum thickness gradient, in the chord-wise direction, also shown in Fig. 6. Although transition is not a point phenomena, its spatial development appeared to be smaller in scale than the chord-wise spacing of experimental profiles. In steady flow, flow visualization clearly showed that the initial stages of the roll-up of two-dimensional vortices were coincident with the sharp increase in momentum thickness.<sup>15</sup> The maximum displacement is, at least, a demarcation between two distinctively different flow regimes.

It was also found that the mean unsteady and steady momentum thickness was nearly the same upstream of maximum displacement thickness. This suggests that the apparent "thinning" of the separated layer in the unsteady mean is simply a displacement of the shear layer toward the wall and is not associated with a broadening of the shear layer. Downstream of turbulent reattachment, about 62% of chord, the mean unsteady momentum thickness remains lower than the steady

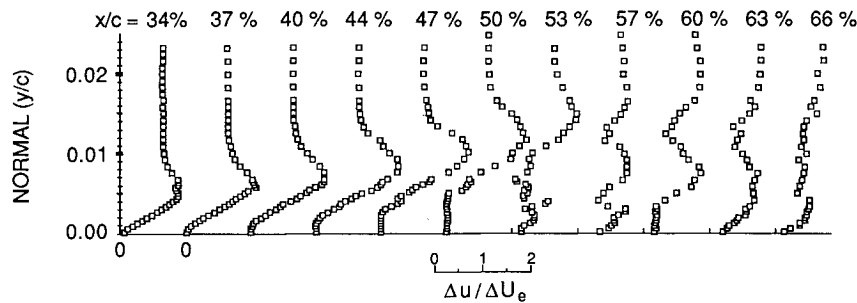


Fig. 7 Fluctuating velocity ratio  $\Delta u/\Delta U_e$  profiles on the Wortmann FX63-137 airfoil ( $\alpha = 7^\circ$ ,  $R_e = 100,000$ ;  $k_c = 0.11$ ,  $A = 7\%$  [ $c = 305$  mm/12 in.]).

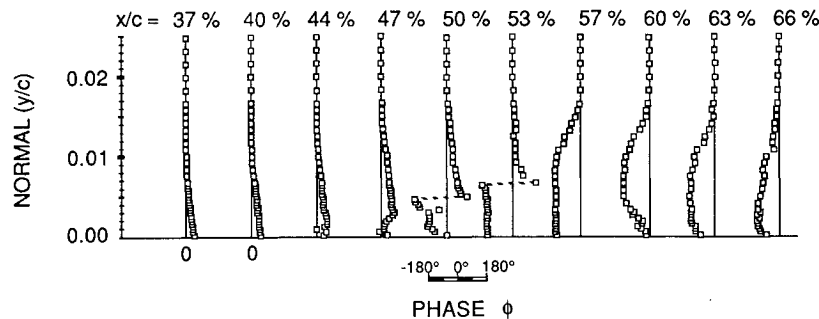


Fig. 8 Phase  $\phi$  profiles on the Wortmann FX63-137 airfoil ( $\alpha = 7^\circ$ ,  $k_c = 0.11$ ;  $R_e = 100,000$ ,  $A = 7\%$  [ $c = 305$  mm/12 in.]).

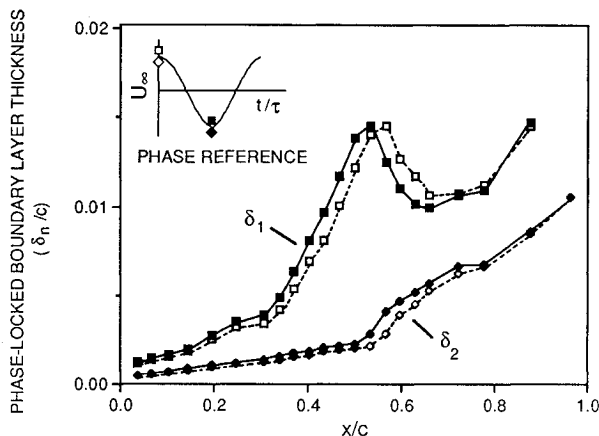


Fig. 9 Phase-locked (minimum and maximum freestream velocity) displacement and momentum thicknesses ( $\alpha = 7^\circ$ ,  $R_e = 100,000$ ;  $k_c = 0.11$ ,  $A = 7\%$  [ $c = 305$  mm/12 in.]; note phase reference to external velocity).

counterpart. This result is significant since a large portion of the airfoil drag results from the boundary layer character downstream of the bubble. For example, the state of the boundary layer at reattachment, in conjunction with the pressure distribution, may influence the location of turbulent separation and size of the airfoil wake.

A plot of the velocity fluctuation ratio  $\Delta u/\Delta U_e$  is shown in Fig. 7. This parameter represents the relative "breathing" of the boundary layer in response to the imposed oscillation. The apparent overshoot in velocity is due to the alternately high and low velocity regions seen by the probe as the boundary layer thickness responds to the oscillating external flow. Unsteady flow in the separated shear layer was associated with larger values of this parameter, relative to an attached boundary layer, and indicated a greater sensitivity to changes in the external velocity.

The phase response of the boundary layer to the periodic flow is shown in Fig. 8. The profiles upstream of, and near separation, had maximum phase leads at the wall that were comparable to phase leads found on the flat plate. This type of behavior is associated with the low momentum (i.e., low iner-

tia) fluid responding to the externally imposed temporal pressure gradient with a greater relative velocity change than high-momentum fluid near the edge of the boundary layer. Downstream of separation, the phase lead became much greater than was observed in the attached laminar boundary layer benchmark case. The sudden phase reversal in the shear layer may be an indication of the initial stages of shear layer roll-up or the location of the zero velocity line. Downstream of the maximum bubble thickness, i.e., transition, the profiles retain a phase lag near to the wall. The extent of the laminar sublayer, where phase lead should occur, was probably too small to detect.

#### Phase-Locked Results

The phase-locked displacement and momentum thickness for the minimum and maximum external velocity are shown in Fig. 9. Upstream of transition, the integrated boundary-layer thicknesses responded to the external oscillation as expected. However, the plot shows that the location of maximum displacement thickness oscillated in the chord-wise direction and that its maximum excursion downstream occurred when the external velocity was nearly a maximum. This is contrary to observed quasisteady behavior of a transitional bubble. An increased Reynolds number should result in a shorter bubble due to transition occurring sooner (i.e., comparable to a critical Reynolds number for transition threshold). In addition, the bubble should be thinner due to less viscous diffusion upstream of separation. In the present data, thinning was observed in the laminar portion of the bubble as indicated by the phase-locked momentum thickness. However, the laminar region appeared to increase in length with increasing external velocity. A micro-computer was used to animate the phase-locked velocity profiles and confirmed the observed behavior in the displacement thickness. In addition, 16-mm flow visualization movies were obtained using the titanium tetrachloride method. The film qualitatively agreed with the trends observed in the phase-locked data.

The equation governing the potential flow at the edge of the boundary layer may be written as

$$\frac{\partial U}{\partial t} + U \frac{\partial U}{\partial x} = - \frac{1}{\rho} \frac{\partial P}{\partial x}$$

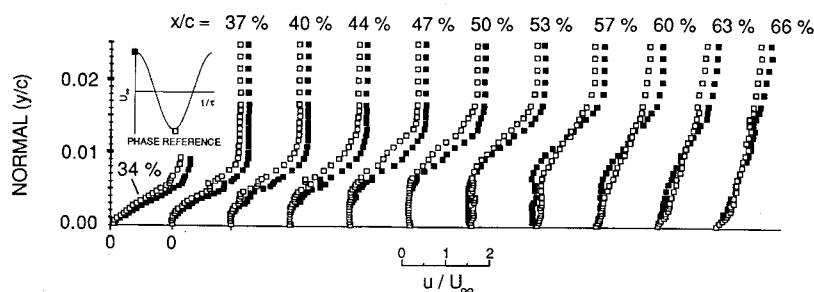


Fig. 10 Phase-locked (minimum and maximum freestream velocity) velocity profiles ( $u/U_\infty$ ) ( $\alpha = 7^\circ$ ,  $R_c = 100,000$ ,  $k_c = 0.11$ ,  $A = 7\%$  [ $c = 305 \text{ mm}/12 \text{ in.}$ ]; note phase reference to external velocity; indicated  $S$ ,  $T$ , and  $R$  are for steady flow).

where the  $x$  direction is assumed tangent to the surface. In steady flow the first term on the left is zero. In the laminar portion of the bubble in steady flow, the stream-wise velocity gradient is nearly zero. This is typical of all separation bubbles. In the unsteady flow, the temporal velocity gradient will dominate in regions of low spatial gradient. Hence, the observed delay of transition could be due to a tendency of the temporally accelerating flow to attenuate the growth of disturbances in the shear layer. Likewise, a decelerating flow may tend to promote "faster" transition such that a "thinner" separated region results.

Figure 10 is a phase-locked plot of the velocity profiles ( $u/U_\infty$ ) at the maximum and minimum external velocity. The instantaneous profiles in the laminar portion of the bubble, upstream of 53% of chord, appear to respond in phase with the external oscillation. Downstream of 53% of chord, the minimum velocity profile begins to fill out faster than the maximum velocity profile. A comparison of profiles at 57, 60, and 63% of chord suggests that the flow is reattaching earlier when the external flow is at a minimum.

More experiments are needed to clarify the flow in the vicinity of reattachment. Velocity vector and Reynolds stress data may help isolate the cause of the observed response of the transitional bubble to an oscillating external flow. A further simplification may be to use uniformly accelerating or decelerating flow.

### Concluding Remarks

Large temporal variations in chord Reynolds number at low-reduced frequencies may produce results contrary to performance characteristics experimentally obtained in steady flow. Pressure distributions in the periodic unsteady flow have revealed an important feature of low Reynolds number aerodynamics that is not usually accounted for in conventional test methods. The appearance of attached or fully separated flow was found to be Reynolds-number-path dependent in contrast to the well known dependence on incidence path. This result is important in the aerodynamic response of flight vehicles that operate in highly unsteady environments. In addition, the results suggest the very different stability characteristics of a transitional bubble as opposed to a separated laminar shear layer with no reattachment.

The influence of this oscillating freestream  $R_c = 100,000$ ;  $k_c = 0.11$ ;  $A = 7\%$ , was confined downstream of, and included, the transitional separation bubble. The two primary observations were:

- 1) The trajectory of the laminar separation was closer to the wall in the mean unsteady flow relative to the steady flow.
- 2) The mean unsteady momentum thickness was less than the steady counterpart downstream of transition.
- 3) Transition appeared to be delayed in accelerating flow, thus producing a transitional bubble that was longest at the maximum external velocity.

Thinning of the separated region in the mean unsteady flow has been observed in both turbulent and laminar separated flows.<sup>16,17</sup> One difference between a "quasisteady" flow and the low-frequency oscillation of the flow presented here was the appearance of periodic vorticity generation due to the temporal pressure gradient imposed on the boundary layer. Also, since the spatial velocity gradient in the laminar portion of the bubble is nearly zero, the temporal velocity gradient dominates and could have been the source of the observed behavior. Finally, the proximity of the separated shear layer to the wall appears to have an impact on the stability characteristics of the flow.<sup>18,15</sup> This, in combination with the temporal pressure gradient, may have suppressed transition when the flow was accelerating and, hence, moved complete transition downstream.

### Acknowledgment

This research was supported by the U.S. Navy Office of Naval Research under contract N00014-83-K-0239 and the Department of Aerospace and Mechanical Engineering, University of Notre Dame. A special thanks to Dr. H. M. Nagib and colleagues at the Illinois Institute of Technology for sharing their experience with unsteady-flow generators.

### References

- <sup>1</sup>Jones, B. M., "Stalling," *R.A.S. Journal*, Vol. 38, No. 285, Sept. 1934, pp. 753-769.
- <sup>2</sup>Jacobs, E. N. and Sherman, A., "Airfoil Section Characteristics as Affected by Variations of the Reynolds Number," NACA TR-586, 1937.
- <sup>3</sup>Schmitz, F. W., "Aerodynamik des Flugmodells, Tragflugelmessungen 1," C. J. E. Volckmann Nachf. E. Wette, Berlin-Charlottenburg 2, 1942 (translated by Redstone Scientific Information Center, U.S. Army Missile Command, Redstone Arsenal, AL, NASA TMX 60976, 1967).
- <sup>4</sup>Mueller, T. J., "Low Reynolds Number Vehicles," AGARDograph 288, Feb. 1985.
- <sup>5</sup>McCroskey, W. J., "Unsteady Airfoils," *Annual Review of Fluid Mechanics*, Vol. 14, 1982, pp. 285-311.
- <sup>6</sup>Ratelle, J. P., "Unsteady Boundary Layer Flow Reversal in a Longitudinally Oscillating Flow," USAF-FJSRL, SRL-TR-78-0006, 1978.
- <sup>7</sup>Saxena, L. S., "An Experimental Investigation of Oscillating Flows Over an Airfoil," Ph.D. Thesis, Illinois Inst. of Technology, 1977.
- <sup>8</sup>Maresca, C. D., et al., "Measurement and Visualization of a Stalling Airfoil in Translational Oscillation," AIAA Paper 79-1519, 1979.
- <sup>9</sup>Brendel, M., "An Experimental Study of the Boundary Layer on a Low Reynolds Number Airfoil in Steady and Unsteady Flow," Ph.D. Thesis, Univ. of Notre Dame, Notre Dame, IN, 1986.
- <sup>10</sup>Karlsson, S. K. F., "An Unsteady Turbulent Boundary Layer," *Journal of Fluid Mechanics*, Vol. 5, Pt. 4, 1960, pp. 622-636.
- <sup>11</sup>Hill, P. G. and Stenning, A. H., "Laminar Boundary Layers in Oscillatory Flow," *Journal of Basic Engineering, Transactions of the ASME*, Sept. 1960, pp. 593-608.

<sup>12</sup>Lighthill, M. J., "The Response of Laminar Skin Friction and Heat Transfer to Fluctuations in the Stream Velocity," *Proceedings of the Royal Society of London, Ser. A*, Vol. 224, No. 1, 1954, pp. 1-23.

<sup>13</sup>Mueller, T. J., "The Influence of Laminar Separation and Transition on Low Reynolds Number Airfoil Hysteresis," *Journal of Aircraft*, Vol. 22, Sept. 1985, pp. 763-770.

<sup>14</sup>Galbraith, R. A. McD., "The Aerodynamic Characteristics of a GU25-5 (11) 8 Aerofoil for Low Reynolds Numbers," *Experiments in Fluids*, Vol. 3, 1985, pp. 253-256.

<sup>15</sup>Mathioulakis, D. S. and Telionis, D. P., "Pulsating Flow Over an

Ellipse at Angle of Attack," AIAA Paper 86-1106, 1986.

<sup>16</sup>Simpson, R. L., Shivaprasad, B. G., and Chew, Y-T, "The Structure of a Separating Turbulent Boundary Layer. Part 4. Effects of Periodic Freestream Unsteadiness," *Journal of Fluid Mechanics*, Vol. 127, 1983, pp. 219-261.

<sup>17</sup>Brendel, M. and Mueller, T. J., "Boundary Layer Measurements on an Airfoil at Low Reynolds Numbers," *Journal of Aircraft* (to be published); also, AIAA Paper 87-0495, 1987.

<sup>18</sup>Betchov, R. and Criminale, W. O., *Stability of Parallel Flows*, Academic Press, New York, 1967, p. 83.

*From the AIAA Progress in Astronautics and Aeronautics Series...*

## **ENTRY VEHICLE HEATING AND THERMAL PROTECTION SYSTEMS: SPACE SHUTTLE, SOLAR STARPROBE, JUPITER GALILEO PROBE—v. 85**

## **SPACECRAFT THERMAL CONTROL, DESIGN, AND OPERATION—v. 86**

*Edited by Paul E. Bauer, McDonnell Douglas Astronautics Company  
and Howard E. Collicott, The Boeing Company*

The thermal management of a spacecraft or high-speed atmospheric entry vehicle—including communications satellites, planetary probes, high-speed aircraft, etc.—within the tight limits of volume and weight allowed in such vehicles, calls for advanced knowledge of heat transfer under unusual conditions and for clever design solutions from a thermal standpoint. These requirements drive the development engineer ever more deeply into areas of physical science not ordinarily considered a part of conventional heat-transfer engineering. This emphasis on physical science has given rise to the name, thermophysics, to describe this engineering field. Included in the two volumes are such topics as thermal radiation from various kinds of surfaces, conduction of heat in complex materials, heating due to high-speed compressible boundary layers, the detailed behavior of solid contact interfaces from a heat-transfer standpoint, and many other unconventional topics. These volumes are recommended not only to the practicing heat-transfer engineer but to the physical scientist who might be concerned with the basic properties of gases and materials.

*Volume 85—Published in 1983, 556 pp., 6 × 9, illus., \$29.95 Mem., \$59.95 List*

*Volume 86—Published in 1983, 345 pp., 6 × 9, illus., \$29.95 Mem., \$59.95 List*

**TO ORDER WRITE: Publications Dept., AIAA, 370 L'Enfant Promenade, SW, Washington, DC 20024**